ORGANIC CHEMISTRY FRONTIERS

CCS 中国化学会 CHINESE CHEMICAL SOCIETY

SIOC

ROYAL SOCIETY OF CHEMISTRY

Effect of Internal Oxygen Substituents on the Properties of Bowl-Shaped Aromatic Hydrocarbons

Journal:	*Organic Chemistry Frontiers*
Manuscript ID	QO-RES-10-2023-001661
Article Type:	Research Article
Date Submitted by the Author:	10-Oct-2023
Complete List of Authors:	Takeo, Yoshihiro; Nagoya University Graduate School of Engineering School of Engineering, Department of Molecular and Macromolecular Chemistry, Graduate School of Engineering Hirano, Junichiro; Nagoya University, Department of Molecular and Macromolecular Chemistry, Graduate School of Engineering Shimizu, Daiki; Kyoto University, Department of Synthetic Chemistry and Biological Chemistry, Graduate School of Engineering Fukui, Norihito; Nagoya University Graduate School of Engineering School of Engineering, Department of Molecular and Macromolecular Chemistry, Graduate School of Engineering Shinokubo, Hiroshi; Nagoya University, Department of Molecular and Macromolecular Chemistry, Graduate School of Engineering

ARTICLE

Effect of Internal Oxygen Substituents on the Properties of Bowl-Shaped Aromatic Hydrocarbons

Yoshihiro Takeo,[a] Junichiro Hirano,[a] Daiki Shimizu,[b] Norihito Fukui*[a,c] and Hiroshi Shinokubo*[a]

Received 00th January 20xx,
Accepted 00th January 20xx

DOI: 10.1039/x0xx00000x

Internally substituted π-systems have remained somewhat underexplored in contrast to their peripherally functionalized counterparts. In this study, we compare a bowl-shaped aromatic hydrocarbon with internal methoxy groups to related derivatives with hydrogen, methyl, and anisyl groups, evaluating their electron-accepting properties, electronic absorption spectra, and fullerene-binding behavior. The methoxy-substituted derivative exhibits enhanced electron-accepting properties and positively shifted electrostatic potential map on its concave surface due to the inductive effect of the oxygen atoms. The σ* orbitals of the internal C–O bonds participate in π-conjugation to change the absorption properties of the bowl-shaped π-skeleton. As hydrocarbons internally substituted with oxygen are key fragments of graphene oxide, these results can be expected to aid the understanding of the structure–property relationships in graphene oxide. Furthermore, internal substitution with oxygen atoms decreases the efficiency of fullerene-binding, thus affording fundamental insights into the design of advanced fullerene-receptors.

Introduction

The functionalization of π-conjugated molecules is a powerful strategy for tuning their structural and electronic properties that is frequently applied in the design of advanced functional materials. Consequently, fundamental research with the aim of understanding the effects of functionalization is essential (Fig. 1). The structure-property relationships upon peripherally functionalizing π-conjugated molecules have been thoroughly investigated and comprehensively understood. In contrast, the effects arising from the functionalization of the internal areas of π-systems have been investigated significantly less due to the small number of internally functionalized π-systems where sp^3 carbon atoms are surrounded by sp^2 carbon atoms.[1–3] Previously reported examples include pyrene **1**, coronene **2**, diindenochrysene **3**, and corannulene derivatives **4** (Fig. 2).[4–18] During the synthesis of *as*-indacenoterrylene, our group synthesized intermediates **5** and **6**, an internally substituted methoxy-*as*-indacenoterrylene derivative and a hydrogen-substituted derivative, respectively.[19] In 2011, Petrukhina and co-workers demonstrated that the absorption maxima of CH_nCl_{3-n}-substituted corannulenium cations **4a–4d** are bathochromically shifted with increasing number of chlorine atoms.[13] However, with the exception of this pioneering work, the influence of the internal substituents of π-conjugated molecules on their properties remains unclear.

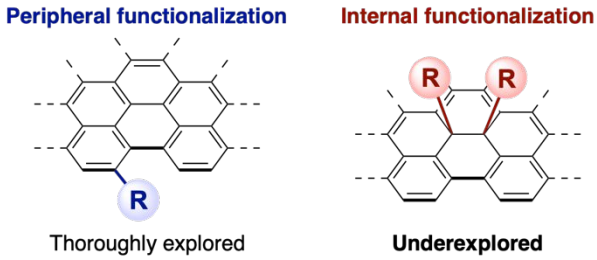

Fig. 1 Peripheral functionalization and internal functionalization of π-conjugated molecules.

Internally functionalized aromatic hydrocarbons can be considered as the fragments of covalently functionalized graphene (CFG).[20] A comprehensive understanding of the impact of internal substituents on the properties of π-conjugated molecules can be expected to aid the design and evaluation of novel CFG-based materials. Of particular interest is the effect of internally substituted oxygen atoms, as hydrocarbons internally substituted with oxygen are key fragments of graphene oxide. Graphene oxide is a typical CFG with numerous applications in e.g., catalysis, visible-light emitting materials, battery electrodes, and (semi)conductors.[21–23]

Moreover, internally functionalized *as*-indacenoterrylene derivatives such as **5** and **6** are ideal for understanding the fundamental structural features that promote fullerene recognition as bowl-shaped π-systems, which often capture fullerene C_{60} on their concave surfaces.[24–34] The peripheral substitution of bowl-shaped π-conjugated cores with electron-donating substituents enhances the association constants for fullerene binding. This behavior had been considered due to increased charge-transfer

[a] *Department of Molecular and Macromolecular Chemistry, Graduate School of Engineering, and Integrated Research Consortium on Chemical Science (IRCCS), Nagoya University, Furo-cho, Chikusa-ku, Nagoya, Aichi 464-8603, Japan. E-mail: fukui@chembio.nagoya-u.ac.jp, hshino@chembio.nagoya-u.ac.jp.*
[b] *Department of Synthetic Chemistry and Biological Chemistry, Graduate School of Engineering, Kyoto University, Nishikyo-ku, Kyoto 615-8510, Japan.*
[c] *PRESTO, Japan Science and Technology Agency (JST), Kawaguchi, Saitama 332-0012, Japan.*

† Electronic Supplementary Information (ESI) available. CCDC 2270012, 2270013, and 2270014. For ESI and crystallographic data in CIF or other electronic format see DOI: 10.1039/x0xx00000x

interactions.[35] However, a theoretical study predicted that peripheral substitution with electron-withdrawing cyano groups would also promote fullerene-binding.[36] This study highlights the substantial contribution of direct dispersion interactions between peripheral substituents and the fullerene to binding the latter, which is consistent with the recent controversy on the nature of π–π interactions.[37–40] A nitrogen-doped bowl-shaped hydrocarbon with *tert*-butyl substituents on its periphery effectively captures fullerene with a high association constant of 3800 M^{-1}, which is approximately ten times larger than association constants for typical corannulene derivatives.[41] Nevertheless, it remains difficult to distinguish the contributions to binding from (i) charge-transfer interactions between the electron-rich π-core and fullerene and (ii) dispersion interactions[42,43] between the bulky *tert*-butyl substituents and the fullerene. Compared to the peripheral functionalization and element-doping strategies, the internal substitution strategy should be advantageous because it enables, via changing the internal substituents, the systematic investigation of the relationship between the electronic structures of the bowl-shaped π-cores and their fullerene binding abilities. Given that the classical Sanders–Hunter model[44] predicts that a decrease of intermolecular electrostatic repulsion between π-electron clouds promotes π-stacking, it is a significant question as to whether or not increasing the electron-donating ability of the bowl-shaped π-core promotes or suppresses fullerene-binding due to competition between the increased charge-transfer interactions and enhanced electronic repulsion.

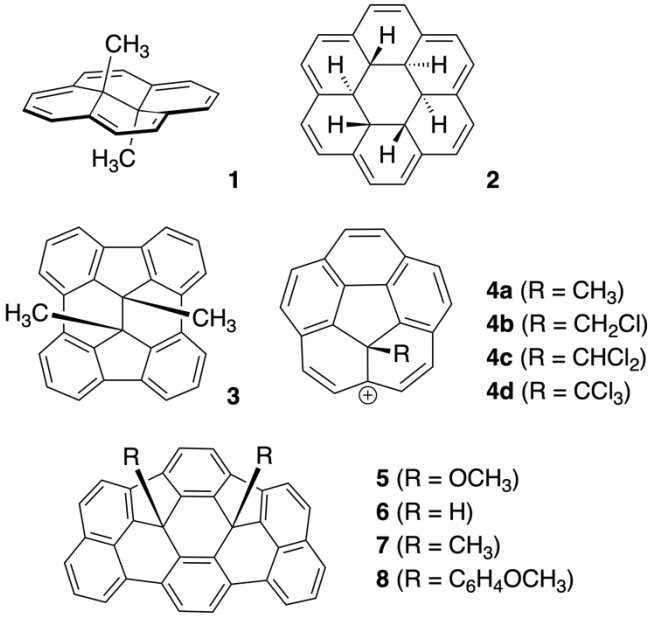

Fig. 2 Internally functionalized π-conjugated molecules.

Results and discussion

Synthesis. We synthesized methyl-substituted derivative **7** and 4-methoxyphenyl-substituted derivative **8** to expand the structural diversity of known *as*-indacenoterrylene derivatives (Scheme 1). Treatment of hydrogen-substituted **6** with butyllithium in THF caused the reaction solution to change from colorless to red, indicating the formation of a lithiated intermediate via deprotonation. The subsequent addition of an excess of iodomethane to the solution afforded methyl-substituted **7** in 51% yield. The molecular structure of **7** was confirmed via a single-crystal X-ray diffraction analysis (Fig. 3). The bowl depth of **7** (2.05 Å) is comparable to those of **5** (1.99 Å) and **6** (1.98 Å) (Fig. S12). Treatment of methoxy-substituted **5** with trifluoromethanesulfonic acid (TfOH) in anisole furnished 4-methoxyphenyl-substituted **8** in 30% yield.

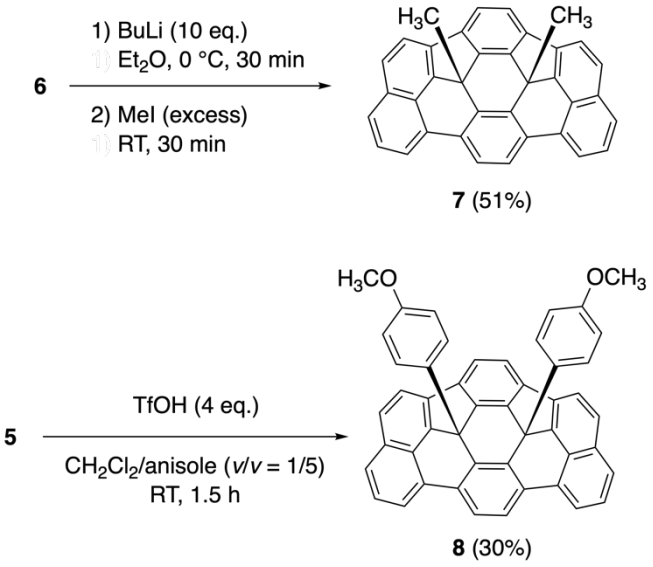

Scheme. 1 Synthesis of methyl-substituted *as*-indacenoterrylene **7** and 4-methoxyphenyl-substituted *as*-indacenoterrylene **8**.

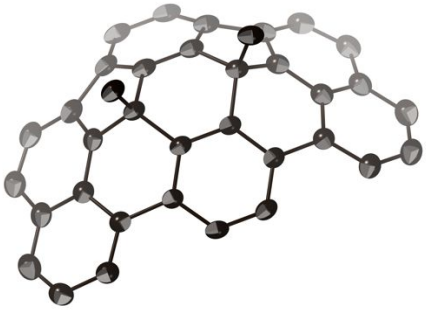

Fig. 3 X-ray crystal structure of **7** with thermal ellipsoids at 50% probability; all hydrogen atoms are omitted for clarity.

Effect of Internal Substituents on the Electronic Properties. The redox potentials of **5**–**8** were measured using cyclic voltammetry in anhydrous CH_2Cl_2 with 0.1 M $[Bu_4N][PF_6]$ as the supporting electrolyte and the $Ag/AgNO_3$ couple as the reference electrode (Fig. S15). The ferrocene/ferrocenium ion couple was used as an internal reference. Compounds **5**–**8** all exhibited one oxidation wave. The oxidation potentials of hydrogen-substituted **6** (0.57 V), methyl-substituted **7** (0.56 V), and 4-methoxyphenyl-substituted **8** (0.61 V) are comparable. On the other hand, the oxygen-substituted methoxy derivative **5** exhibits a significantly higher oxidation potential (0.75 V). These results indicate that internal oxygen-based substituents act as electron-withdrawing groups.

The UV/vis absorption spectra of **5**–**8** were measured in CH_2Cl_2 (Fig. 4). The tails of the absorption spectra extend to approximately 520 nm, indicating that the HOMO–LUMO gaps of **5**–**8** are also comparable. However, the spectral shapes in the 300–450 nm range differ. Hydrogen-substituted **6** and methyl-substituted **7** exhibit intense absorptions with vibrational bands, while the absorption band of 4-methoxyphenyl-substituted **8** is relatively broad. Importantly, methoxy-substituted **5** displays two peaks at 313 and 339 nm, which originate from extended conjugation through the σ* orbitals of the C–O bonds (*vide infra*).

To gain further insight into the electronic properties of **5**–**8**, density-functional-theory (DFT) calculations were performed at the B3LYP/6-31G(d) level. The optimized structures of **5**–**8** are similar, indicating that any structural changes caused by the internal substituents are negligible (Fig. S20). As shown in Fig. 5a, the HOMO–LUMO gaps of **5**–**8** are comparable (3.00–3.05 eV), and these values are in good agreement with the optical HOMO–LUMO gaps estimated from the UV/vis absorption spectra. The distribution of these orbitals is similar regardless of the internal substituents, except for the HOMO–1 in **8**, which is localized on the electron-rich 4-methoxyphenyl group (Fig. S19).

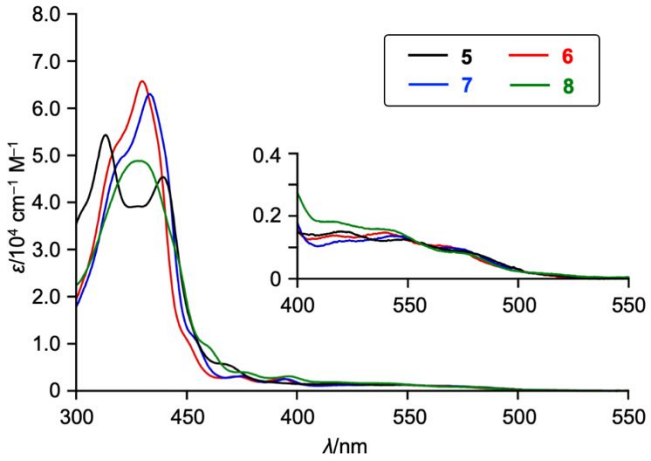

Fig. 4 UV/vis absorption spectra of **5**-**8** in CH_2Cl_2; λ = wavelength; ε = extinction coefficient.

In sharp contrast to the HOMO–LUMO gaps, we found a difference between the energy levels of the molecular orbitals of methoxy-substituted **5** and **6**–**8**. The energy levels of the frontier orbitals of methoxy-substituted **5** are by 0.13–0.19 eV lower than those of **6**–**8**, which agrees well with their observed redox behavior. The enhanced electron-accepting ability of **5** can be attributed to the inductive effect of the oxygen atoms. Furthermore, the LUMO+1 level of **5** is by 0.34–0.38 eV more stable than those of **6**–**8**. The orbital distributions on the concave surfaces of **5** and **6** are shown in Fig. 5b. In the case of the hydrogen-substituted **6**, the π-conjugation is disrupted at the internal sp^3 carbons. On the other hand, the LUMO+1 of methoxy-substituted **5** exhibits substantial orbital coefficients at the internal sp^3 carbons due to the C–O σ* orbitals. These results indicate that the presence of internal oxygen-based substituents in π-conjugated molecules results in enhanced electron-accepting ability, firstly via an inductive effect and secondly via π-extension through the C–O σ* orbitals. This conclusion stands in sharp contrast to the effect that peripheral oxygen-based substituents on π-conjugated systems often act as electron-donating groups due to the dominance of the mesomeric effect.

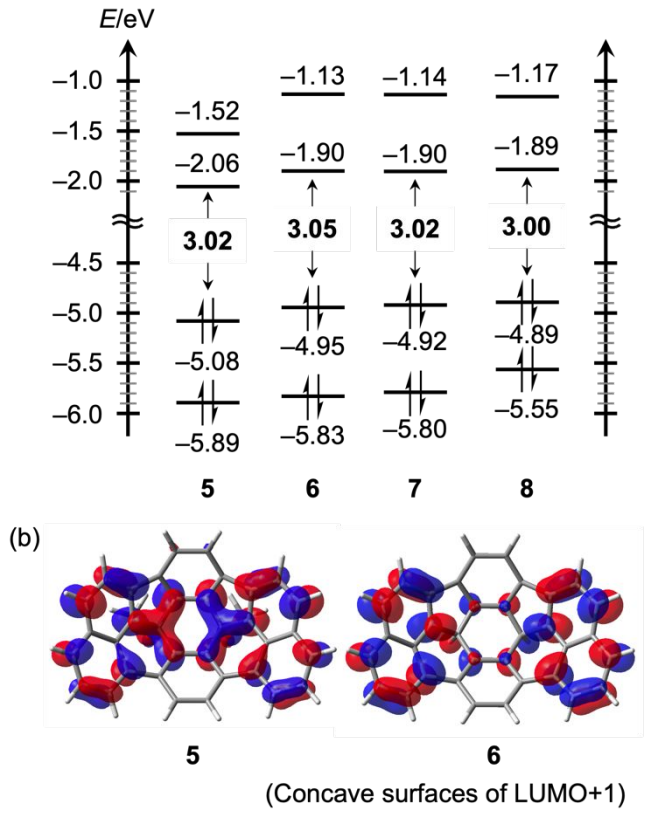

Fig. 5 (a) Energy diagrams for **5**-**8**. (b) Orbital distributions on the concave surfaces of the LUMO+1 of **5** and **6**. DFT calculations were performed at the B3LYP/6-31G(d) level; isovalue = 0.03.

The electrostatic potential maps of the internally functionalized *as*-indacenoterrylene derivatives **5**–**8** and the peripherally functionalized benzene derivatives C_6H_5R (R = H, CH_3, OCH_3, F, and CN) are shown in Fig. 6. Methoxy-substituted **5** has a less negative concave surface than **6**–**8**. This trend stands in contrast with that observed for the peripherally functionalized benzene molecules, where anisole has a more negative π-surface than benzene. The electrostatic potential of the concave surface of **5** is comparable to that of fluorobenzene. The relatively positive concave surface of **5** can be attributed to the dominance of the inductive effect of the oxygen atoms.

Time-dependent DFT (TD-DFT) calculations performed on **5**–**8** at the B3LYP/6-31G(d) level were able to reproduce their experimentally obtained absorption spectra (Figs. S22–S25). The simulated absorption spectrum of methoxy-substituted **5** exhibited two allowed transitions at 309 and 339 nm with oscillator strengths of 0.59 and 0.27, respectively. A natural-transition-orbital (NTO) analysis of **5** suggested that: (1) the orbital contribution in the absorption band at 339 nm is the same as that of hydrogen-substituted **6** at 326 nm; and (2) the absorption band at 309 nm contains the contribution of the transition to the LUMO+1 (Figs. S22 and S23). In the case of **6**-**8**, the oscillator strengths of the absorption bands with contributions to the transition to LUMO+1

are lower than 0.15. These results indicate that the emergence of a new absorption band in the electronic spectrum of **5** should be attributed to π-extension through the σ* orbitals of the C–O bonds.

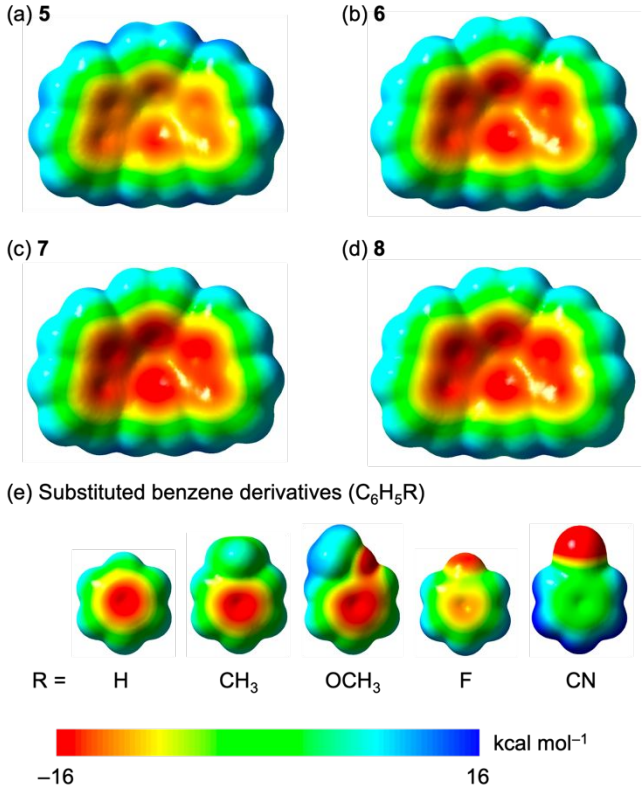

Fig. 6 Electrostatic potential maps of (a) **5**, (b) **6**, (c) **7**, (d) **8**, and (e) the peripherally substituted benzene derivatives. The concave surfaces of *as*-indacenoterrylene derivatives **5**–**8** are shown. Calculations were conducted at the B3LYP/6-31G(d) level.

Effect of the Internal Substituents on Fullerene-Binding. We conducted fullerene-binding experiments on hydrogen-substituted **6** in toluene-d_8 at 303 K. The addition of C_{60} to the solution of **6** resulted in changes of the ^{1}H NMR chemical shifts, indicating the formation of a host–guest complex (Fig. 7a). The signals for the peripheral protons (a, f, and g) and the internally substituted hydrogens (h) were down-field shifted upon addition of C_{60}. A Job's plot analysis confirmed the formation of a 1:1 complex (Fig. 7b). Co-crystallization of **6** with C_{60} produced single crystals consisting of a 1:1 ratio of **6** and C_{60}, in which C_{60} is located on both the concave and convex surfaces of **6** (Fig. 7d). The interplanar distances between **6** and C_{60} are 3.18 Å for the concave surface and 3.27 Å for the convex surface.

To determine the structure of the host–guest complex C_{60}@**6** in solution, we used DFT calculations to simulate the ^{1}H NMR signals of two possible arrangements (concave–C_{60} and convex–C_{60}) (Table S8). These calculations predicted that the signal of proton (g) would shift down-field in the concave–C_{60} arrangement and up-field in the convex–C_{60} arrangement. Consequently, we concluded that **6** captures C_{60} on the concave surface, as is typically seen in bowl-shaped π-systems.

We measured the ^{1}H NMR spectra of **6** in the presence of C_{60} while varying the amount of C_{60} added (Fig. S27). The curve fitting yielded an association constant of 918 ± 72 M^{-1} (Fig. 7c), which is higher than that of 1,3,5,7,9-pentakis(4-methoxyphenylthio)corannulene (454 ± 72 M^{-1}).[28] We also determined association constants at different temperatures (313 K: 713 ± 60 M^{-1}; 323 K: 606 ± 56 M^{-1}; 333 K: 518 ± 55 M^{-1}; 343 K: 425 ± 51 M^{-1}; Table S10). These values were plotted using the Eyring equation to provide an enthalpy change (ΔH) of –16.1 kJ mol^{-1} and an entropy change (ΔS) of 3.5 J K^{-1} mol^{-1} (Fig. S30).

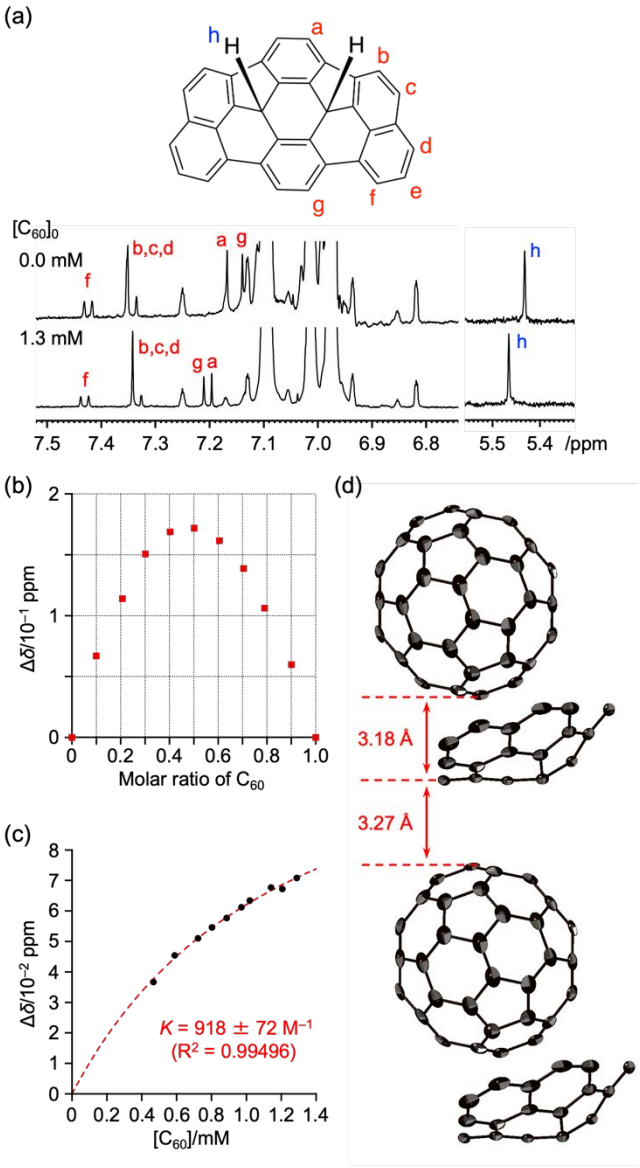

Fig. 7 (a) ^{1}H NMR spectra of **6** and [**6** + C_{60}] in toluene-d_8 ([**6**]$_0$ = 0.16 mM). (b) Job's plot of $\Delta\delta$ at position g versus the molar ratio of C_{60} in toluene-d_8 at 303 K ([**6**]$_0$ + [C_{60}]$_0$ = 0.6 mM). (c) Plot of $\Delta\delta$ at position g versus [C_{60}] at 303 K ([**6**]$_0$ = 1.6 × 10^{-4} M). (d) Crystal packing of C_{60}@**6** with thermal ellipsoids at 50% probability.

The binding properties of **5**, **7**, and **8** with C_{60} were also investigated (Figs. S26, S28, S29 and Tables S9, S11, S12). An X-ray diffraction analysis of C_{60}@**5** indicated that **5** captures C_{60} on the concave surface (Fig. S13). The thermodynamic parameters ΔH and ΔS were obtained from ^{1}H NMR titrations (Table 1). The ΔH values all lie within a range of 3.6 kJ mol^{-1} of one another. Nevertheless,

the Δ*H* value of methoxy-substituted **5** is approximately 3 kJ mol^{-1} higher than those of **6**-**8**.

Table 1. Thermodynamic parameters for the binding of fullerene with **5**-**8**.

	K [M^{-1}][a]	*ΔH* [kJ mol^{-1}]	*ΔS* [J K^{-1} mol^{-1}]
5	884 ± 46	–13.6	11.6
6	918 ± 72	–16.1	3.5
7	865 ± 15	–16.5	1.4
8	964 ± 14	–17.2	0.3

[a] Association constant in toluene-d_8 at 303 K.

We also conducted a second-generation energy decomposition analysis on C_{60}@**5** and C_{60}@**6** at the ωB97M-V/def2-TZVPPD level using absolutely localized molecular orbitals (ALMO-EDA)[45] (Table 2).[46] The total energy gains upon fullerene-binding were found to be –121.85 kJ mol^{-1} for C_{60}@**5** and –123.39 kJ mol^{-1} for C_{60}@**6**. The difference between these total energies (1.5 kJ mol^{-1}) nicely accords with the experimental results. The electrostatic interaction (ΔE_{elec}), Pauli repulsion (ΔE_{Pauli}), and dispersion force (ΔE_{disp}) mutually offset each other, resulting in comparable frozen interaction values (ΔE_{elec} + ΔE_{Pauli} + ΔE_{disp} = –94.13 kJ mol^{-1} for C_{60}@**5**; –94.80 kJ mol^{-1} for C_{60}@**6**). The polarization energies (ΔE_{pol}) of C_{60}@**5** (–13.30 kJ mol^{-1}) and C_{60}@**6** (–13.46 kJ mol^{-1}) are also similar. Conversely, the stabilization by charge-transfer interactions (ΔE_{CT}) in C_{60}@**6** is 2.06 kJ mol^{-1} higher than that in C_{60}@**5**.

The ΔE_{Pauli} value of C_{60}@**5** is smaller than that of C_{60}@**6**, which accords with the expectation given by the Sanders–Hunter model:[44] the decreased electron density on the concave surface of an *as*-indacenoterrylene core suppresses the repulsion between π-electrons. The decreased electron repulsion also enhances the solvation with toluene before complexation with C_{60}, which nicely accords with the observed tendency that methoxy-substituted **5** exhibited a larger Δ*S* value than those of **6**, **7**, and **8**. However, in the point of enthalpy upon fullerene recognition, the energetical advantage due to the decrease of electronic repulsion has been offset by other interactions (ΔE_{elec}, ΔE_{disp}, ΔE_{CT}). Consequently, the introduction of electron-withdrawing oxygen atoms in a bowl-shaped *as*-indacenoterrylene core slightly hampers the fullerene recognition.

Table 2. Energy decomposition analysis for C_{60}@**5** and C_{60}@**6**.[a]

	ΔE_{elec}	ΔE_{Pauli}	ΔE_{disp}	ΔE_{pol}	ΔE_{CT}	ΔE_{tot}
C_{60}@**5**	–152.51	243.56	–185.86	–13.30	–13.74	–121.85
C_{60}@**6**	–155.61	248.57	–187.09	–13.46	–15.80	–123.39

[a] In units of kJ mol^{-1}.

Conclusions

We have investigated the impact of internal substituents in four internally functionalized *as*-indacenoterrylene derivatives (**5**–**8**) on their electron-accepting properties, electronic absorption spectra, and fullerene-binding behavior. Methoxy-substituted **5** was found to be a stronger electron acceptor than the other derivatives due to the inductive effect of the oxygen atoms. π-Conjugation in **5** is facilitated through the σ* orbitals of the internal C–O bonds, resulting in the emergence of a new absorption band in the UV/vis spectrum. As hydrocarbons internally substituted with oxygen are key fragments of graphene oxide, these results improve our understanding of the structure–property relationships of graphene oxide. We have furthermore demonstrated that **5** exhibits a positively shifted electrostatic potentials on its concave surface due to internal oxygen substitution. The fullerene-binding of **5** has been energetically unfavorable compared to **6**, **7**, and **8**, as a result of complex compensation among ΔE_{elec}, ΔE_{Pauli}, ΔE_{disp}, and ΔE_{CT}. These results afford fundamental insights that can be expected to aid the design of advanced fullerene receptors.

Author Contributions

The manuscript was written through contributions of all authors. All authors have approved of the final version of the manuscript. H.S. and N.F. designed and conducted the project and finalized the manuscript. T.Y. carried out all the experiments including the synthesis and characterization. J.S. supported the data collection. D.S. conducted a second-generation energy decomposition analysis.

Conflicts of interest

There are no conflicts to declare.

Acknowledgements

This work was supported by JSPS KAKENHI grants JP20H05863, JP20H05867, and JP22K14663 as well as JST, PRESTO grant JPMJPR21Q7 (Japan). Computational resources were provided by the Super Computer System, Institute for Chemical Research, Kyoto University (Japan).

Notes and references

1 V. Boekelheide, Intrusion of substituents into the cavity of aromatic π-electron clouds. *Pure Appl. Chem.* 1975, **44**, 751–765.
2 L. T. Scott, H. E. Bronstein, D. V. Preda, R. B. M. Ansems, M. S. Bratcher and S. Hagen, Geodesic polyarenes with exposed concave surfaces. *Pure Appl. Chem.* 1999, **71**, 209–219.
3 L. T. Scott, Chemistry at the interior atoms of polycyclic aromatic hydrocarbons. *Chem. Soc. Rev.* 2015, **44**, 6464–6471.
4 V. Boekelheide and J. B. Phillips, Aromatic Molecules Bearing Substituents within the Cavity of the π-Electron Cloud. Synthesis of *trans*-15,16-Dimethyldihydropyrene. *J. Am. Chem. Soc.* 1967, **89**, 1695–1704.

5 R. H. Mitchell and V. Boekelheide, Syntheses of [2.2]metacyclophane-1,9-diene and *trans*-15,16-dihydropyrene. *J. Am. Chem. Soc.* 1970, **92**, 3510–3512.

6 R. H. Mitchell and V. Boekelheide, Transformation of sulfide linkages to carbon-carbon double bond. Syntheses of *cis*- and *trans*-15,16-dimethyldihydropyrene and *trans*-15,16-dihydropyrene. *J. Am. Chem. Soc.* 1974, **96**, 1547–1557.

7 T. Yamato, A. Miyazawa and M. Tashiro, Metacyclophanes and related compounds. 22. Medium-sized cyclophanes. Preparation and valence tautomerism of 8,16-disubstituted [2.2]metacyclophane-1,9-dienes. *J. Org. Chem.* 1992, **57**, 266–270.

8 R. H. Mitchell, T. R. Ward, Y. Chen, Y. Wang, S. A. Weerawarna, P. W. Dibble, M. J. Marsella, A. Almutairi and Z.-Q. Wang, Synthesis and Photochromic Properties of Molecules Containing [e]-Annelated Dihydropyrenes. Two and Three Way π-Switches Based on the Dimethyldihydropyrene − Metacyclophanediene Valence Isomerization. *J. Am. Chem. Soc.* 2003, **125**, 2974–2988.

9 R. B. DuVernet, T. Otsubo, J. A. Lawson and V. Boekelheide, Additions and Corrections - Bridged [18]Annulenes. Dependency of the Ring Current Contribution to Chemical Shift on the Contour of the Annulene Perimeter. *J. Am. Chem. Soc.* 1975, **97**, 6607–6608.

10 T. Otsubo, R. Gray and V. Boekelheide, Bridged [18]annulenes. 12b,12c,12d,12e,12f,12g-Hexahydrocoronene and its mono- and dibenzo analogs. Ring-current contribution to chemical shifts as a measure of degree of aromaticity. *J. Am. Chem. Soc.* 1978, **100**, 2449–2456.

11 W. Huber, J. Lex, T. Meul and K. Müllen, *trans*-15,16-Dimethyl-1,4:8,11-ethanediylidene[14]annulene. *Angew. Chem., Int. Ed. Engl.* 1981, **20**, 391–393.

12 D. V. Preda and L. T. Scott, Addition of dihalocarbenes to corannulene. A fullerene-type reaction. *Tetrahedron Lett.* 2000, **41**, 9633–9637.

13 A. V. Zabula, S. N. Spisak, A. S. Filatov, A. Y. Rogachev and M. A. Petrukhina, A Strain-Releasing Trap for Highly Reactive Electrophiles: Structural Characterization of Bowl-Shaped Arenium Carbocations. *Angew. Chem., Int. Ed.* 2011, **50**, 2971–2974.

14 H. E. Bronstein and L. T. Scott, Fullerene-like Chemistry at the Interior Carbon Atoms of an Alkene-Centered $C_{26}H_{12}$ Geodesic Polyarene. *J. Org. Chem.* 2008, **73**, 88–93.

15 N. Ngamsomprasert, Y. Yoshida, Y. Yakiyama, N. Ikuma and H. Sakurai, Nucleophilic Substitution at the Internal Carbon of Sumanene Framework with Inversion of Configuration. *Chem. Lett.* 2018, **47**, 878–880.

16 H.-W. Ip, C.-F. Ng, H.-F. Chow and D. Kuck, Three-Fold Scholl-Type Cycloheptatriene Ring Formation around a Tribenzotriquinacene Core: Toward Warped Graphenes. *J. Am. Chem. Soc.* 2016, **138**, 13778–13781.

17 W.-S. Wong, W.-W. Lau, Y. Li, Z. Liu, D. Kuck and H.-F. Chow, Scholl-Type Cycloheptatriene Ring Closure of 1,4,9,12-Tetraarylfenestrindanes: Reactivity and Selectivity in the Construction of Fenestrane-Based Polyaromatic Saddles. *Chem.-Eur. J.* 2020, **26**, 4310–4319.

18 H. Y. Cho, R. B. M. Ansems and L. T. Scott, Site-selective covalent functionalization at interior carbon atoms and on the rim of circumtrindene, a $C_{36}H_{12}$ open geodesic polyarene. *Beilstein J. Org. Chem.* 2014, **10**, 956–968.

19 Y. Tanaka, N. Fukui and H. Shinokubo, *as*-Indaceno[3,2,1,8,7,6-*ghijklm*]terrylene as a near-infrared absorbing C_{70}-fragment. *Nat. Commun.* 2020, **11**, 3873.

20 V. Georgakilas, M. Otyepka, A. B. Bourlinos, V. Chandra, N. Kim, K. C. Kemp, P. Hobza, R. Zboril and K. S. Kim, Functionalization of Graphene: Covalent and Non-Covalent Approaches, Derivatives and Applications. *Chem. Rev.* 2012, **112**, 6156–6214.

21 H. Bai, C. Li and G. Shi, Functional Composite Materials Based on Chemically Converted Graphene. *Adv. Mater.* 2011, **23**, 1089–1115.

22 D. Chen, H. Feng and J. Li, Graphene Oxide: Preparation, Functionalization, and Electrochemical Applications. *Chem. Rev.* 2012, **112**, 6027–6053.

23 S. Eigler and A. Hirsh, Chemistry with Graphene and Graphene Oxide—Challenges for Synthetic Chemists. *Angew. Chem., Int. Ed.* 2014, **53**, 7720–7738.

24 E. M. Pérez and N. Martín, Curves ahead: molecular receptors for fullerenes based on concave–convex complementarity. *Chem. Soc. Rev.* 2008, **37**, 1512–1519.

25 T. Kawase and H. Kurata, Ball-, Bowl-, and Belt-Shaped Conjugated Systems and Their Complexing Abilities: Exploration of the Concave−Convex π−π Interaction. *Chem. Rev.* 2006, **106**, 5250–5273.

26 M. Saito, H. Shinokubo and H. Sakurai, Figuration of bowl-shaped π-conjugated molecules: properties and functions. *Mater. Chem. Front.* 2018, **2**, 635–661.

27 M. C. Stuparu, Corannulene: A Curved Polyarene Building Block for the Construction of Functional Materials. *Acc. Chem. Res.* 2021, **54**, 2858–2870.

28 S. Mizyed, P. E. Georghiou, M. Bancu, B. Cuadra, A. K. Rai, P. Cheng and L. T. Scott, Embracing C_{60} with Multiarmed Geodesic Partners. *J. Am. Chem. Soc.* 2001, **123**, 12770–12774.

29 A. Sygula, F. R. Fronczek, R. Sygula, P. W. Rabideau and M. M. Olmstead, A Double Concave Hydrocarbon Buckycatcher. *J. Am. Chem. Soc.* 2007, **129**, 3842–3843.

30 M. Yanney, F. R. Fronczek and A. Sygula, A 2:1 Receptor/C_{60} Complex as a Nanosized Universal Joint. *Angew. Chem., Int. Ed.* 2015, **54**, 11153–11156.

31 L. N. Dawe, T. A. AlHujran, H.-A. Tran, J. I. Mercer, E. A. Jackson, L. T. Scott and P. E. Georghiou, Corannulene and its penta-tert-butyl derivative co-crystallize 1 : 1 with pristine C60-fullerene. *Chem. Commun.* 2012, **48**, 5563–5565.

32 M. C. Stuparu, Rationally Designed Polymer Hosts of Fullerene. *Angew. Chem., Int. Ed.* 2013, **52**, 7786–7790.

33 K. Ikemoto, R. Kobayashi, S. Sato and H. Isobe, Entropy-Driven Ball-in-Bowl Assembly of Fullerene and Geodesic Phenylene Bowl. *Org. Lett.* 2017, **19**, 2362–2365.

34 Y.-M. Liu, D. Xia, B.-W. Li, Q.-Y. Zhang, T. Sakurai, Y.-Z. Tan, S. Seki, S.-Y. Xie and L.-S. Zheng, Functional Sulfur-Doped Buckybowls and Their Concave–Convex Supramolecular

Assembly with Fullerenes. *Angew. Chem., Int. Ed.* 2016, **55**, 13047–13051.

35 P. E. Georghiou, A. H. Tran, S. Mizyed, M. Bancu and L. T. Scott, Concave Polyarenes with Sulfide-Linked Flaps and Tentacles: New Electron-Rich Hosts for Fullerenes. *J. Org. Chem.* 2005, **70**, 6158–6163.

36 D. Josa, J. Rodríguez-Otero, E. M. Cabaleiro-Logo, L. A. Santos and T. C. Ramalho, Substituted Corannulenes and Sumanenes as Fullerene Receptors. A Dispersion-Corrected Density Functional Theory Study. *J. Phys. Chem. A* 2014, **118**, 9521–9528.

37 S. Grimme, Do Special Noncovalent π–π Stacking Interactions Really Exist? *Angew. Chem., Int. Ed.* 2008, **47,** 3430–3434.

38 M. O. Sinnokrot and C. D. Sherrill, Substituent Effects in π−π Interactions: Sandwich and T-Shaped Configurations. *J. Am. Chem. Soc.* 2004, **126**, 7690–7697.

39 E. C. Lee, D. Kim, P. Jurečka, P. Tarakeshwar, P. Hobza and K. S. Kim, Understanding of Assembly Phenomena by Aromatic −Aromatic Interactions: Benzene Dimer and the Substituted Systems. *J. Phys. Chem. A* 2007, **111**, 3446–3457.

40 S. E. Wheeler and K. N. Houk, Substituent Effects in the Benzene Dimer are Due to Direct Interactions of the Substituents with the Unsubstituted Benzene. *J. Am. Chem. Soc.* 2008, **130**, 10854–10855.

41 H. Yokoi, Y. Hiraoka, S. Hiroto, D. Sakamaki, S. Seki and H. Shinokubo, Nitrogen-embedded buckybowl and its assembly with C60. *Nat. Commun.* 2015, **6**, 8215.

42 P. R. Schreiner, L. V. Chernish, P. A. Gunchenko, E. Y. Tikhonchuk, H. Hausmann, M. Serafin, S. Schlecht, J. E. P Dahl, R. M. K. Carlson and A. A. Fokin, Overcoming lability of extremely long alkane carbon–carbon bonds through dispersion forces. *Nature* 2011, **477**, 308–311.

43 L. Yang, C. Adam, G. S. Nichol and S. L. Cockroft, How much do van der Waals dispersion forces contribute to molecular recognition in solution? *Nat. Chem.* 2013, **5**, 1006–1010.

44 C. A. Hunter and J. K. M. Sanders, The Nature of π–π Interaction. *J. Am. Chem. Soc.* 1990, **112**, 5525–5534.

45 P. R. Horn, Y. Mao and M. Head-Gordon, Probing non-covalent interactions with a second generation energy decomposition analysis using absolutely localized molecular orbitals. *Phys. Chem. Chem. Phys.* 2016, **18**, 23067–23079.

46 N. Mardirossian and M. Head-Gordon, ω B97M-V: A combinatorially optimized, range-separated hybrid, meta-GGA density functional with VV10 nonlocal correlation. *J. Chem. Phys.* 2016, **144**, 214110.